Available online at www.sciencedirect.com

ScienceDirect

Polymer 48 (2007) 1212–1218

polymer

www.elsevier.com/locate/polymer

Effect of particle size on the mechanical properties of polystyrene and poly(butyl acrylate) core/shell polymers

L.A. Pérez-Carrillo [a], M. Puca [a], M. Rabelero [a], K.E. Meza [a], J.E. Puig [a], E. Mendizábal [a,*], F. López-Serrano [b], R.G. López [c]

[a] *Departamentos de Química e Ingeniería Química, Universidad de Guadalajara, M. García Barragán 1451, Guadalajara, Jalisco 44430, Mexico*
[b] *Facultad de Química, Universidad Nacional Autónoma de México, México, D.F. 04510, Mexico*
[c] *Centro de Investigación en Química Aplicada, Saltillo, Coah. 25253, Mexico*

Received 6 September 2006; received in revised form 1 January 2007; accepted 2 January 2007
Available online 8 January 2007

Abstract

The effects of particle size and polymer location (core or shell) on the mechanical properties of core/shell materials composed of polystyrene (PST) and poly(butyl acrylate) (PBA) made by a two-stage emulsion or microemulsion polymerization process are reported. Low-seed content (LSC) latexes were made by batch polymerization in microemulsions stabilized with DTAB in the presence of an organic salt (dibutyl phosphite). High-seed content (HSC) latexes were produced by microemulsion or emulsion polymerization in semi-continuous process. These latexes were subsequently used to form core/shell particles of PST/PBA or PBA/PST and their mechanical properties were examined and compared. Our results indicate that core/shell particle size and the location of the polymers have important effects on the mechanical properties.

Keywords: Core/shell polymer; Particle size; Mechanical properties

1. Introduction

Core/shell polymers are attracting scientific and industrial interest because their chemical and mechanical properties can be tailored for applications such as paints, adhesives, paper and textile manufacturing, and impact modifiers [1–7]. Moreover, these materials have better properties than those of the parent polymers [8–10]. Core/shell polymers are usually made by emulsion polymerization in a two-stage process; first one monomer is polymerized to form the core, then the second monomer is added in batch or semi-continuously and polymerized over the seed particles to form the shell [11,12]. One of the polymers has a much lower glass transition temperature (T_g) and the other a higher T_g than the temperature at which the material is being used [11–13]. By microemulsion polymerization it is also possible to produce core/shell polymer particles but with smaller sizes than those obtained by emulsion polymerization [14,15]. Aguiar et al. reported that core/shell of polystyrene (PST) and poly(butyl acrylate) (PBA) made by microemulsion polymerization had higher Young's modulus and tenacity than the core/shell polymers with similar composition made by conventional emulsion polymerization because of their smaller particle size [15].

In emulsion polymerization final particle size can be modified by the addition of salts [16–20]. Full et al. reported that smaller polystyrene particles were produced by polymerizing in microemulsions containing electrolytes compared to those obtained in their absence, and that smaller particles were produced as the salt content was increased [21]. In this work we investigated the effects of particle size and polymers' location and composition on the mechanical properties of core/shell of PST and PBA made by a two-stage emulsion or microemulsion polymerization process in order to contribute to the understanding of the relationship between morphology and

---

* Corresponding author. Tel.: +52 3336199920; fax: +52 3336194028.
E-mail address: lalomendizabal@hotmail.com (E. Mendizábal).

0032-3861/$ - see front matter © 2007 Elsevier Ltd. All rights reserved.
doi:10.1016/j.polymer.2007.01.001

properties with the aim to produce materials with tailored properties. Our results indicate that core/shell particle size as well as polymer composition and location have important effects on the mechanical properties of core/shell materials.

2. Experimental section

Dodecyltrimethylammonium bromide (DTAB) and cetyltrimethylammonium bromide (CTAB), both 99%+ pure from Tokyo Kasei, were re-crystallized from a 50/50 (v/v) acetone/ethanol mixture. Styrene and butyl acrylate, 99% pure from Scientific Polymer Products (SPP), were passed through a TR-7 or a HR-4 column (SPP) to remove their inhibitors. Allyl methacrylate (ALMA), 98% pure from Aldrich, was used as crosslinking agent and compatibilizer. 2,2′-Azobis(2-amidinopropane) hydrochloride (V-50) from Wako Chem. was purified by re-crystallization from methanol. Dibutyl phosphite (DBP), 96% pure from Aldrich, and hydroquinone, 99% pure from Productos Químicos Monterrey, were used as received. Doubly distilled and de-ionized water was employed.

Core/shell polymers were made in a 200-mL three neck glass reactor. First, low-seed content (LSC) latexes of PST or PBA were produced by the polymerization at 60 °C in microemulsions containing 14.4 wt.% DTAB, 4 wt.% styrene or butyl acrylate with small amount of ALMA ($w_{\mathrm{ALMA}}/w_{\mathrm{monomer}} = 0.01$), and 81.6 wt.% of a 0.15 M DBP aqueous solution, using V-50 ($w_{\mathrm{V\text{-}50}}/w_{\mathrm{monomer}} = 0.01$) as initiator. High-seed content (HSC) latexes of PST and PBA (∼40 wt.% solids) were obtained by adding more monomer semi-continuously to the LSC latex made without DBP. Also, HSC latexes of PST and PBA with larger particle sizes were made by the polymerization of 1 wt.% CTAB, 10 wt.% monomer (and $w_{\mathrm{ALMA}}/w_{\mathrm{monomer}} = 0.01$) and 88.86 wt.% water emulsion, initiated with V-50 ($w_{\mathrm{V\text{-}50}}/w_{\mathrm{monomer}} = 0.01$) at 60 °C, followed by the semi-continuous addition of more monomer. Before adding the other monomer to form the shell, the emulsion (EMU) and microemulsion (HSC) latexes were diluted with water to 10 wt.% solids. In the second stage, the needed amount of BA (or ST) was added semi-continuously to form the shell over the PST (or PBA) seeds made by either of the process described above. The reacting system was continuously stirred and sparged with argon throughout the reaction. After the reaction, the polymer was precipitated from the latex by adding excess methanol, filtered, washed to eliminate adsorbed surfactant and un-reacted monomer, and dried in a vacuum oven to constant weight.

Particle size was measured with a Malvern 4700C QLS apparatus at room temperature. Intensity correlation data were analyzed by the method of cumulants to provide the average decay rate, $\langle \Gamma \rangle$, ($= 2q^2D$, where D is the diffusion coefficient and q is the magnitude of the scattering vector). The measured diffusion coefficients were represented in terms of the apparent radii using Stokes' law and the assumption that the solvent has the viscosity of water. Lattices were diluted up to 1000 times before QLS measurements to minimize particle–particle interactions.

The latex particles were examined in a JEOL 1010 transmission electron microscope (TEM) at an accelerating voltage of 100 kV to determine their shape and microstructure. To improve the contrast, samples were treated with a 1% phosphotungstic acid solution for 2 h, deposited over copper grids and allowed to dry at room temperature for 24 h before TEM examination.

Glass transition temperatures (T_g) were obtained with cooling and heating rates of 10 °C/min after one heating- and cooling scan to eliminate thermal history, with a Q100 differential scanning calorimeter of TA instruments.

Polymer bars (10 × 63 × 2 mm) for tensile tests were made by heating at 120 °C and pressing at 150 bar in a hydraulic press for 40 min. Tensile tests were performed at room temperature according to the ASTM D-638 method at an elongation velocity of 2 in/min in a universal testing machine (United). Impact tests were performed following the ASTM D-1709 method in a CS-126G Custom Scientific instrument. The dart employed to test the PST-rich samples weighed 285 g while the one used for the PBA-rich probes weighed 920 g. Tensile stress–strain, hardness and impact data are the average of at least three independent measurements.

3. Results

Table 1 shows the conversions at the end of stages 1 and 2 for the hard-core/soft-shell and soft-core/hard-shell polymers studied here. Independent of the monomer used to form the seeds, the procedure of synthesis, core/shell composition and polymers' location, the final conversions at the end of first and second stages are high, especially when compared to polymers of low T_g such as hexyl and butyl methacrylates [22].

Table 2 shows the z-average particle size (D_{Pz}) measured by QLS for the different core/shell polymer formulations prepared here. At the end of the first stage, LSC latexes with small particles (23–25 nm) were obtained. This table also shows that the seed particles of the HSC microemulsion-made latexes at the end of the first stage (ca. 40 nm) are larger than those of the LSC latexes but still within the typical size range obtained in microemulsion polymerization [23,24]. As

Table 1
Conversions at the end of stages 1 and 2

Core/shell composition	Synthesis procedure	Conversion (%)	
		Stage 1	Stage 2
PST/PBA 40/60	LSC	93	93
PST/PBA 40/60	HSC	94	94
PST/PBA 40/60	EMU	92	86
PBA/PST 40/60	LSC	94	86
PBA/PST 40/60	HSC	96	91
PBA/PST 40/60	EMU	94	90
PST/PBA 60/40	LSC	93	91
PST/PBA 60/40	HSC	94	95
PST/PBA 60/40	EMU	89	87
PBA/PST 60/40	LSC	99	87
PBA/PST 60/40	HSC	96	96
PBA/PST 60/40	EMU	94	92

Table 2
Average particle size at the end of stages 1 and 2

Core/shell composition	Synthesis procedure	D_{Pz} (nm)		
		Stage 1	Stage 2	Stage 2 estimated
PST/PBA 40/60	LSC	23.5 ± 0.9	29.0 ± 1.5	31.9
PST/PBA 40/60	HSC	47.3 ± 2.4	59.2 ± 6.7	63.9
PST/PBA 40/60	EMU	162.0 ± 7.2	210.0 ± 18.9	218.0
PBA/PST 40/60	LSC	24.6 ± 1.1	28.5 ± 2.2	30.5
PBA/PST 40/60	HSC	41.7 ± 3.7	53.8 ± 5.1	56.6
PBA/PST 40/60	EMU	209.7 ± 18.3	278.1 ± 25.7	282.3
PST/PBA 60/40	LSC	22.7 ± 0.9	28.9 ± 1.5	26.3
PST/PBA 60/40	HSC	42.0 ± 3.1	45.8 ± 5.3	49.5
PST/PBA 60/40	EMU	194.3 ± 22.9	221.3 ± 19.4	226.8
PBA/PST 60/40	LSC	24.9 ± 1.5	27.5 ± 1.9	25.9
PBA/PST 60/40	HSC	41.7 ± 4.3	49.9 ± 4.8	50.1
PBA/PST 60/40	EMU	209.7 ± 20.6	241.3 ± 22.1	248.4

expected, the seed latexes made by emulsion polymerization have the largest sizes (Table 2). Average particle sizes are larger at the end of the second stage independent of the process employed to prepare the PST or PBA seeds. This growth suggests that the monomer added during the second stage polymerizes over the seed particles to form a core/shell structure. However, this growth does not exclude the formation of other morphologies or additional homo-polymer particles.

To infer indirectly that the second monomer was incorporated over the seed particles, we estimated the final diameter assuming that all the monomers added in the second stage were used to cover uniformly the seeds and that the seed particles have the same diameter (equal to D_{Pz}). For the calculations, it was taken into consideration the degree of conversion in both stages. Table 2 shows the final experimental diameters, measured by QLS, and the estimated diameters. In most cases they are similar indicating that almost all the monomers added in the second stage were incorporated to the seed particles.

DSC detected two glass transitions (thermograms are not shown) indicating the presence of two segregated phases: one at −50 to −45 °C due to PBA and other at ca. 100 °C due to PST.

TEM confirmed the core/shell morphology. Fig. 1 depicts pictures of the LSC (a), HSC (b) and EMU (c) latexes of PBA/PST (40/60 w/w), where the light and dark domains correspond to the PBA and PST regions, respectively. Here, because of the order of addition (PBA was polymerized in the first stage to produce the seeds), PST is clearly in the outer domain of the structured polymer forming the shell. However, when styrene was polymerized in the first stage to produce the seeds and PBA was added in the second stage, some phase inversion occurs because the minimum interfacial free energy for this situation corresponds to the inverted core/shell morphology [25]. This is observed in Fig. 2 for PST/PBA (40/60 w/w), where incomplete inverted core/shell morphology is observed.

Fig. 3 shows the stress−strain curves for the LSC, HSC and EMU core/shell polymers with PST/PBA weight ratio of 40/60, where PST was used as the seed. Notice that the polymer

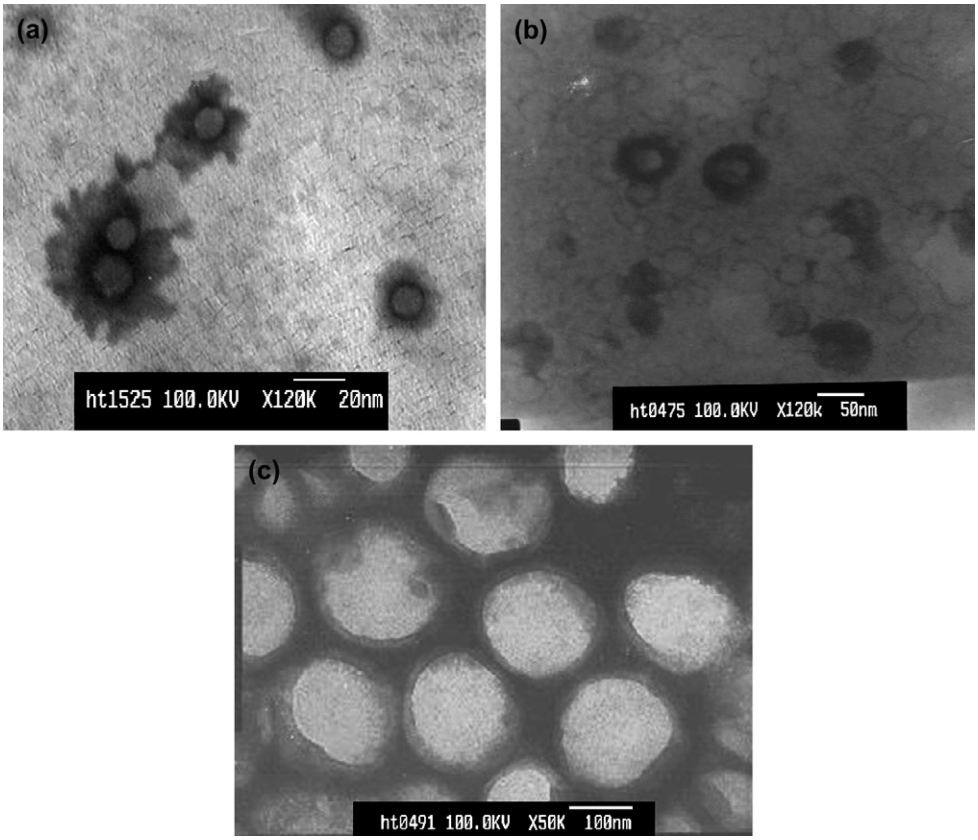

Fig. 1. TEM photographs of PBA/PST core/shell particles (40/60 w/w) prepared by different methods: (a) LSC; (b) HSC; (c) EMU.

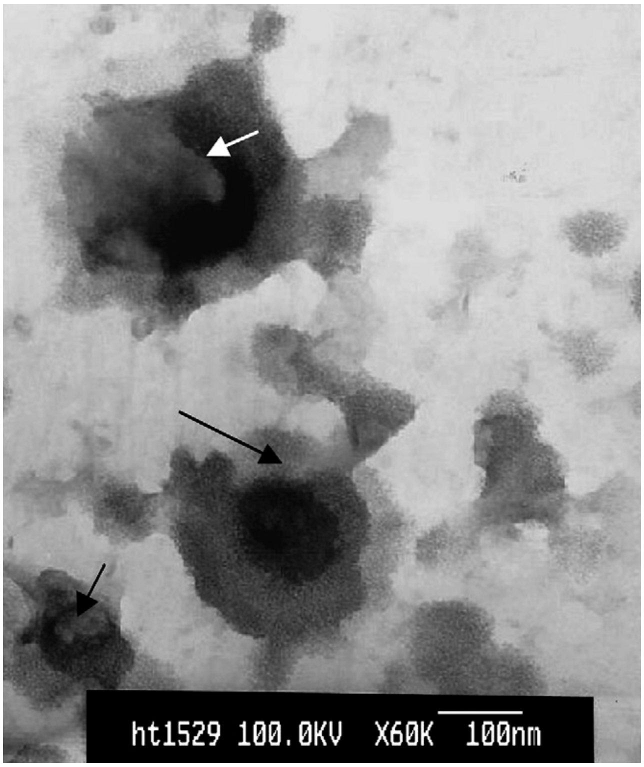

Fig. 2. TEM photography of PST/PBA core/shell particles (40/60 w/w) made by batch emulsion polymerization. Arrows indicate the phase inversion locations.

becomes more rigid and exhibits higher yield stress and smaller elongation at break as the core/shell particle size decreases.

Fig. 4 depicts stress–strain curves for the LSC, HSC and EMU core/shell polymers with PST/PBA weight ratio of 60/40 using again PST as the seed. Because these polymers have higher PST content their behavior approximates more to that of a rigid plastic. Also, as particle size decreases, the modulus increases. The LSC core/shell polymer has a very low elongation and breaks before yielding. The HSC polymer exhibits a higher elongation and a smaller tensile strength. The EMU polymer, in turn, yields at lower elongations than the HSC one but it has a slightly higher tensile strength.

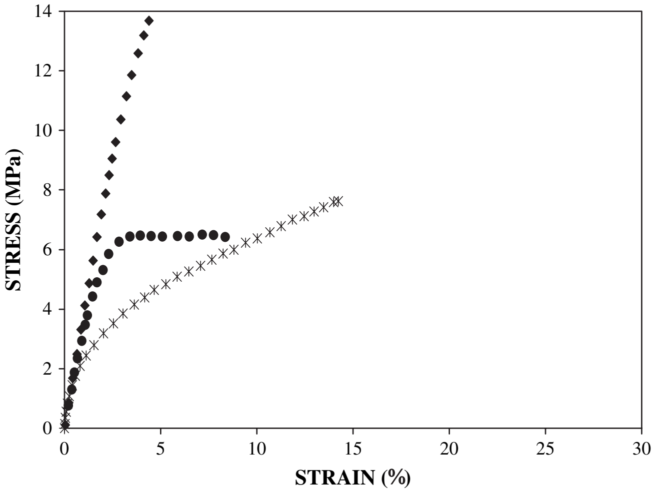

Fig. 4. Stress–strain curves of core/shell polymers with PST/PBA weight ratio of 60/40 made with different polymerization processes: LSC (◆), HSC (●) and EMU (⁎).

Fig. 5 shows stress–strain data for the LSC, HSC and EMU core/shell polymers with PBA/PST weight ratio of 40/60 but with PBA particles as the seeds. All the polymers are rigid and break before yielding with elongations at break smaller than 5%.

Fig. 6 presents the stress–strain results for the LSC, HSC and EMU core/shell polymers with PBA/PST weight ratio of 60/40 made using PBA as the seed. All the polymers have low ultimate strength and large elongation before breaking. All of them present yield stress, followed by a region of strain hardening and finally failure. However, now as particle size increases the polymers have a larger tensile strength.

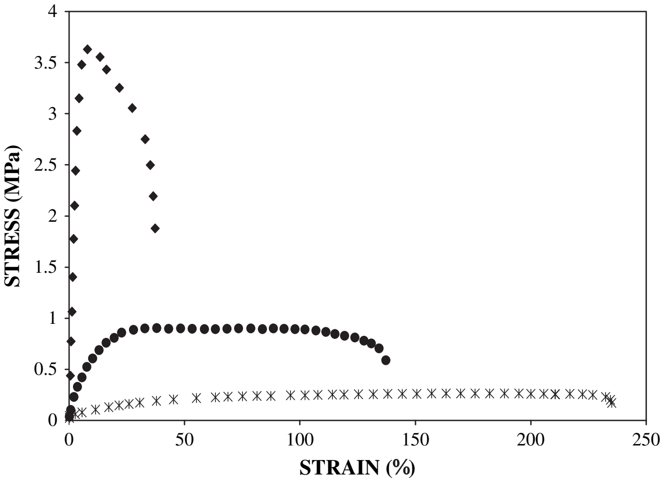

Fig. 3. Stress–strain curves of core/shell polymers with PST/PBA weight ratio of 40/60 made with different polymerization processes: LSC (◆), HSC (●) and EMU (⁎).

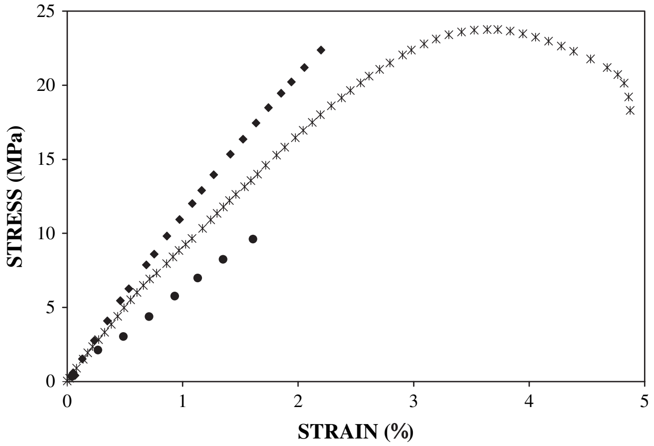

Fig. 5. Stress–strain curves of core/shell polymers with PBA/PST weight ratio of 40/60 made with different polymerization processes: LSC (◆), HSC (●) and EMU (⁎).

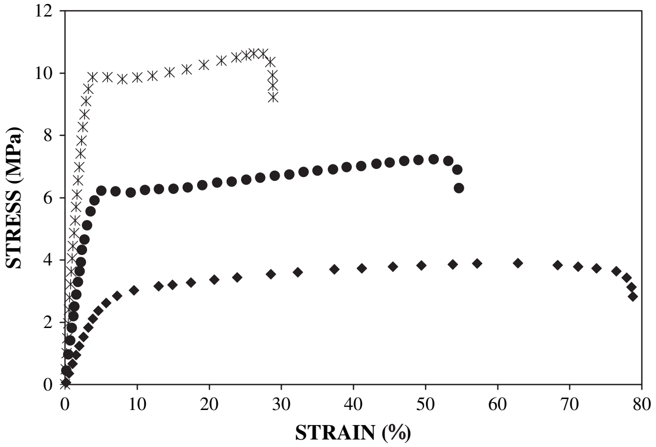

Fig. 6. Stress–strain curves of core/shell polymers with PBA/PST weight ratio of 60/40 made with different polymerization processes: LSC (◆), HSC (●) and EMU (✱).

Table 3 shows the Young's modulus, tensile strength and impact energy for the LSC, HSC and EMU core/shell polymers. Notice that the mechanical properties are sensitive to particle size for polymers with identical composition.

4. Discussion

Core/shell polymers of polystyrene and poly(butyl acrylate) can be obtained with high conversions (Table 1) and controlled particle size (Table 2) by microemulsion or emulsion polymerization. Particle size was regulated by batch microemulsion polymerization to produce LSC latexes ($D_{\mathrm{Pz}} \sim 30$ nm), by semi-continuous microemulsion polymerization to produce HSC latexes ($D_{\mathrm{Pz}} \sim 50$ nm) or by semi-continuous emulsion polymerization to yield EMU latexes ($D_{\mathrm{Pz}} \sim 200$ nm) (Table 2).

Particle growth at the end of the second stage (Table 2) and the detection of two glass transition temperatures at ca. −50 and 100 °C suggest the formation of the core/shell morphology. The PBA-core/PST-shell morphology is confirmed by TEM when PBA is used as the seed and styrene is added in the second stage (Fig. 1). Moreover, the particle size estimated from TEM (Fig. 1) is similar to that measured by QLS considering the differences between these techniques, inasmuch as QLS measures an intensity-weighed diameter whereas TEM provides directly the number- and volume-average diameters. However, when PST forms the seeds and BA polymerizes in the second stage, the minimum interfacial free energy change corresponds to the inverted core/shell structure and so, some phase inversion should occur [25,26]. Fig. 2 shows that this is the case since incomplete inverted core/shell morphology is observed.

Our results (Figs. 3–6 and Table 3) indicate that the mechanical properties strongly depend on particle size and polymer location (core or shell). Polymers containing 60 wt.% PBA (Figs. 3 and 6) behave more as rubbery materials exhibiting small tensile modulus, low tensile strength, large ultimate elongation and high impact resistance, regardless whether the PBA is on the core or the shell (according to the order of addition of monomers during the preparation method). By contrast, the polymers rich in PST (60 wt.%) behave more as plastics with larger Young's modulus and lower elongations at break, regardless of the location of PST (Figs. 4 and 5).

The comparison of the mechanical properties of polymers with similar composition reveals that superior properties are obtained when the shell is made of the hard material, indicating that the shell plays an important role in determining these properties. For blends with droplet–matrix morphology it was reported that the tensile modulus is largely determined by the modulus of the matrix phase, in agreement with results obtained here [27].

The comparison between polymers with the same composition but polymerized under different conditions (Table 3 and Figs. 3–6) demonstrates that the mechanical properties depend on particle size. Core/shell polymers with different particle sizes but with similar composition ratio and polymer location (core or shell) have different mechanical properties probably because of the differences in specific surface area and shell thickness.

Fig. 7 shows cartoons of core/shell polymers as a function of core/shell ratio and particle size, estimated with the assumptions that the particles are spherical and mono-dispersed and that all of the second monomer is incorporated evenly on the particles that form the core. In this figure it is evident that the shell becomes increasingly thinner as the core/shell polymers' ratio increases because the particle's volume augments

Table 3
Mechanical properties as a function of composition and preparation method

Core/shell composition	Synthesis procedure	*E* (MPa)	Tensile strength (MPa)	Ultimate elongation (%)	Impact energy (J/cm)
PST/PBA 40/60	LSC	85.0 ± 8.9	3.0 ± 0.26	37.2 ± 2.1	28.9 ± 3.1
PST/PBA 40/60	HSC	10.9 ± 1.3	0.9 ± 0.01	137.3 ± 15.1	24.0 ± 2.3
PST/PBA 40/60	EMU	0.5 ± 0.027	0.3 ± 0.04	235.1 ± 21.1	47.0 ± 5.1
PBA/PST 40/60	LSC	1125 ± 38.9	22.4 ± 2.7	2.2 ± 0.23	0.81 ± 0.12
PBA/PST 40/60	HSC	606.1 ± 22.9	9.5 ± 0.05	1.7 ± 0.19	0.7 ± 0.59
PBA/PST 40/60	EMU	916.7 ± 30.6	23.8 ± 3.5	4.9 ± 0.39	1.25 ± 0.12
PST/PBA 60/40	LSC	383.3 ± 35.6	13.7 ± 0.95	4.4 ± 0.28	0.37 ± 0.03
PST/PBA 60/40	HSC	312.5 ± 24.1	6.5 ± 0.50	9.4 ± 1.21	0.27 ± 0.29
PST/PBA 60/40	EMU	171.4 ± 21.4	7.6 ± 0.21	14.2 ± 1.34	0.83 ± 0.11
PBA/PST 60/40	LSC	57.5 ± 5.8	3.9 ± 0.42	78.7 ± 4.7	17.1 ± 1.53
PBA/PST 60/40	HSC	178.6 ± 31.3	7.2 ± 0.43	54.5 ± 5.3	11.9 ± 1.42
PBA/PST 60/40	EMU	440.0 ± 34.0	10.6 ± 0.84	28.8 ± 3.4	21.4 ± 2.09

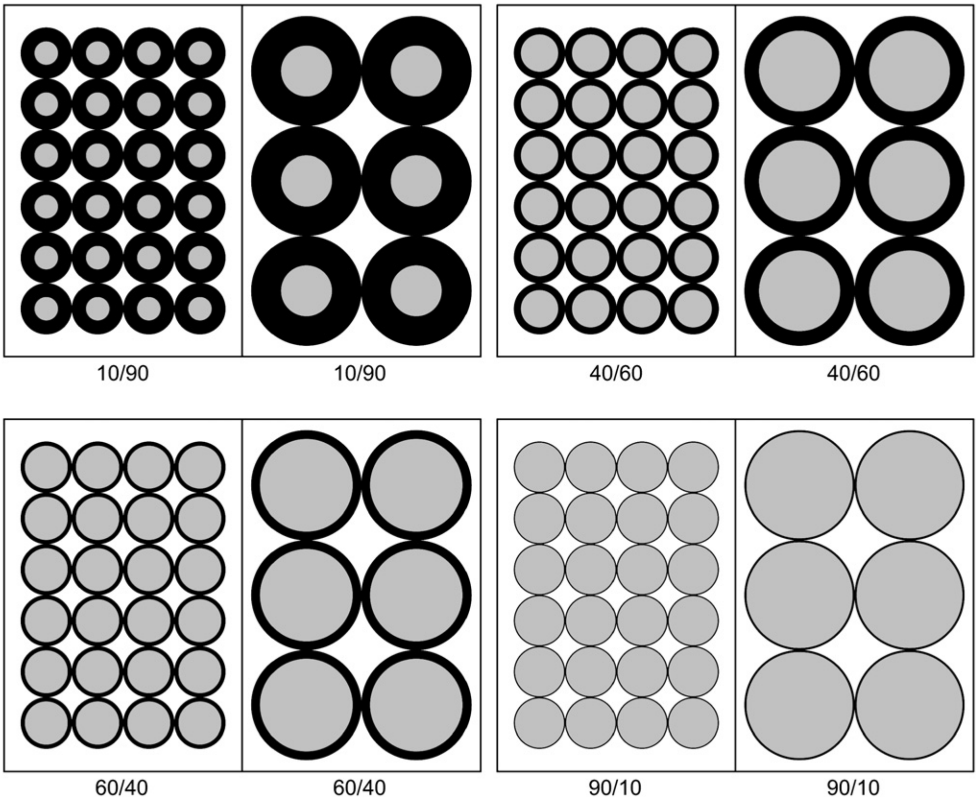

Fig. 7. Cartoons of core/shell morphology as a function of size and composition.

as the third power of the radius; moreover, the calculations disclose that for large ratios, the shell becomes so thin that the properties of the polymer are dominated by those of the polymer that forms the core.

When the shell is made of the rubbery polymer, the material becomes more rigid as particle size decreases (Figs. 3 and 4 and Table 3) because the PBA layer becomes increasingly thinner (Table 2), which causes the rigid cores to be closer, giving as a result a better transmission of the stress, which contributes to increase the material strength. This is more evident for the particles with the lower PBA content because of the thinner shell (Fig. 4). In addition, Schwarzl et al. [28] reported that in rock salt–urethane rubber composites, the tensile strength increases from 3.8×10^5 to 12.6×10^5 N/m^2 as the rock particles decrease from 300–480 nm to 33–40 nm because of the increase in interfacial area per unit of volume of filler and because the stress concentration increases with particle size, so the probability of finding a large flaw within the volume increases.

However, when the shell is made of the rigid PST, the material becomes more rigid as particle size increases because the shell thickness increases (Table 2). This effect is more noticeable for the particles with the lower PST content (40%), because when the particles have a larger PST content in the shell (60%), the modulus and tensile strength of the smaller particles approach that of the PST, giving as a result only a small increase in these properties as the shell thickness increases for larger PST-to-PBA ratios. It has been reported that the tensile strength increases as particle size increases in blends of spherical particles–rubber matrix [28–30]. For polyblends, it has been reported that the size of rubbery particles in a brittle matrix has an important effect on their stress–strain behavior: the modulus, elongation to yield and yield stress decrease as the size of the rubbery particles increases [31]. Because the core/shell morphology resembles polyblends of rubbery particles in a brittle matrix, this report confirms our results. In addition, because the thermodynamically preferred morphology for the polystyrene–poly(butyl acrylate) pair is that with the PST located in the shell [32], when PST is used as the seed and butyl acrylate is the second-stage monomer, PST will tend to diffuse into the shell. Hence, when the second-stage monomer is butyl acrylate, the larger the relative amount of PST that should diffuse to the shell as the particles become smaller due to the thinner shell thickness (see Fig. 7), giving as a result more rigid materials, in agreement with our results (Table 3). Okubo [33] reported that the mode of addition of the second monomer (monomer absorption versus drop-wise methods) influences the degree of phase inversion when inverted core/shell structures are thermodynamically favored, because of diffusion limitations and the high viscosity of the reacting medium. Hence, in our case only partial inversion occurred for the PST/PBA particles, which explains the lower mechanical properties of the PST/PBA particles compared to the ''thermodynamically favored'' PBA/PST particles. Aguiar et al. [15] reported that core/shell of PST/PBA polymers made by emulsion polymerization (larger particles) has lower modulus, lower tensile strength and higher elongation at break than the microemulsion-made polymers (smaller particles) with the same composition, in agreement with our results.

Impact strength increases with the rubbery content independent of the location (core or shell) of the rubbery phase (Table 3). When the shell is made of the rubbery material the larger the particle size the larger the impact strength because the shell layer is thicker and it can dissipate more energy by mechanical damping. By contrast, when the rubbery phase is forming the core, there is a small increase in impact strength with increasing particle size. Donald and Kramer [34–36] reported that the impact strength increases with particle size up to a limit for blends consisting of a rubbery-dispersed phase in brittle matrix.

5. Concluding remarks

In summary, the synthesis of core/shell particles by emulsion and microemulsion polymerization allows the control of particle size and, as a consequence, a variety of mechanical properties can be obtained. The mechanical properties of the core/shell polymers are strongly influenced by the particle size through the shell thickness and by the nature (T_g) and location of the composing polymers.

Acknowledgement

The National Council of Science and Technology of Mexico (CONACYT) supported this work (grant # 38725-U). One of us (L.A.P.C.) acknowledges the scholarship from CONACYT.

References

[1] Henry F, Cansell F, Guillamine JL, Pichot C. Colloid Polym Sci 1989; 267:167.
[2] Gerli A, Berkhout S, Cardoso X. Pulp Paper Europe 2002; (May/June).
[3] Bertelo C, Meunier G, Lermite A, Dargelos P, Drujon X. U.S. Patent RE37,851; September 17, 2002.
[4] Mendizábal E, Hernández-Patiño PJ, Puig JE, Canché-Escamilla G, Katime I, Castaño V. J Appl Polym Sci 1999;74:3299–304.
[5] Wang GJ, Kang CS, Jin RG. Prog Org Coat 2004;50:55–61.
[6] Zerafati S, Tran M, Quoc B, Gruat N, Granel C. European Patent EP1207172; May 2002.
[7] Ferguson CJ, Russell GT, Gilbert RG. Polymer 2002;43:6371–82.
[8] Rios L, Hidalgo M, Cavaille JY, Guillot J, Guyot A, Pichot C. Colloid Polym Sci 1991;269:812–24.
[9] Lee S, Rudin A. In: Daniels E, Sudol ED, El-Aasser MS, editors. Polymer latexes. ACS Symposium Series, vol. 492; 1992. p. 234.
[10] Hidalgo M, Cavaille JY, Cabane B, Chevalier Y, Guillot J, Rios L, et al. Polym Adv Technol 1995;6:296–300.
[11] Hidalgo M, Cavaille JY, Guillot J, Guyot A, Pichot C, Rios L, et al. Colloid Polym Sci 1992;270:1208–21.
[12] Ha JW, Park LJ, Kim DK. Macromolecules 2002;35:6811–8.
[13] Jonsson JE, Karlsson OJ, Hassander H, Tornell B. Macromolecules 2001; 34(5):1512.
[14] Hentze H-P, Kaler EW. Curr Opin Colloid Interface Sci 2003;8(2):164.
[15] Aguiar A, González-Villegas S, Rabelero M, Mendizábal E, Puig JE. Macromolecules 1999;32:6767–71.
[16] Blackley DC. Emulsion polymerization: theory and practice. New York: Wiley; 1975.
[17] Blackley DC, Sebastian SAR. Br Polym J 1989;21:313.
[18] Dunn AS, Said ZFM. Polymer 1982;23:1172.
[19] Matsumoto T. In: Lissant KJ, editor. Emulsions and emulsion technology, vol. 6. New York: Marcel Decker; 1974. p. 474. Part II.
[20] Tsvetkov NS, Yurzhenko AI. Colloid J 1956;18:351.
[21] Full AP, Kaler EW, Arellano J, Puig JE. Macromolecules 1996;29:2764.
[22] Co CC, de Vries R, Kaler EW. Macromolecules 2001;34:3224–32.
[23] Puig JE. In: Salamone JP, editor. Polymeric materials encyclopedia, vol. 6. Boca Raton: CRC Press; 1996. p. 4333–41.
[24] Candau F. In: Kumar P, Mittal KL, editors. Handbook of microemulsion science and technology. New York: Marcel Dekker; 1999. p. 679.
[25] Zhao K, Sun P, Liu D, Wang L. J Appl Polym Sci 2004;92:3144–52.
[26] Sundberg DC, Casassa AP, Pantazopoulos J, Muscato MR. J Appl Polym Sci 1990;41:1425–42.
[27] Willemse RC, Speijer A, Langeraar AE, Posthuma de Boer A. Polymer 1999;40:6645–50.
[28] Schwarzl FR, Bree HW, Nederveen CJ. In: Lee EH, editor. Proceedings of the fourth international congress on rheology, vol. 3. New York: Wiley; 1965. p. 241.
[29] Liepie A, Adicoff A. J Appl Polym Sci 1972;16:1115.
[30] Gent AN. J Mater Sci 1980;15:2884.
[31] Baer M. J Appl Polym Sci 1972;16:1109.
[32] Rabelero M, López-Cuenca S, Puca M, Mendizábal E, Esquena J, Solans C, et al. Polymer 2005;46:6182–91.
[33] Okubo M. Makromol Chem Macromol Symp 1990;35–36:307.
[34] Donald AM, Kramer EJ. J Appl Polym Sci 1982;27:3729.
[35] Bragaw CG. Adv Chem Ser 1971;99:86.
[36] Bender BW. J Appl Polym Sci 1965;9:2887.